

The Design of Polymer Planar Optical Triplexer with MMI Filter and Directional Coupler

Vítězslav JEŘÁBEK, Karel BUŠEK, Václav PRAJZLER, David MAREŠ, Rudolf SVOBODA

Dept. of Microelectronics, Czech Technical University, Technická 2, 168 27 Prague, Czech Republic

jerabek@fel.cvut.cz

Abstract. *Optical bidirectional WDM transceiver is a key component of the Passive Optical Network of the Fiber to the Home topology. Essential parts of such transceivers are filters that combine multiplexing and demultiplexing function of optical signal (triplexing filters). In this paper we report about a design of a new planar optical multi-wavelength selective system triplexing filter, which combines a multimode interference filter with directional coupler based on the epoxy polymer SU-8 on Si/SiO₂ substrate. The optical triplexing filter was designed using the Beam Propagation Method. The aim of this project was to optimize the triplexing filter optical parameters and to minimize the planar optical wavelength selective system dimensions. The multimode interference filter was used for separation of downstream optical signal in designed optoelectronic integrated WDM transceiver. The directional coupler was used for adding of upstream optical signal.*

materials and accordingly the cost of them was higher. Therefore there is a strong demand to develop new approach to realize such elements using new materials but the same time assuring the properties comparable with the reported ones [5-10]. It means easy fabrication process, which would allow mass production and low cost of the required devices.

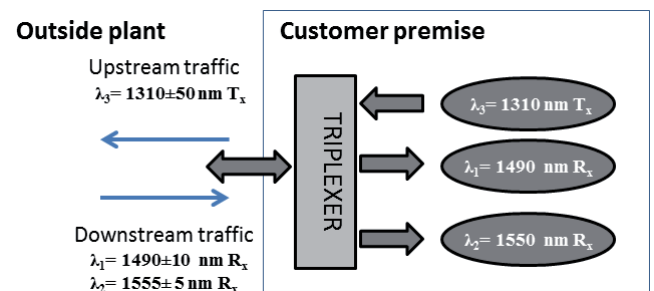


Fig. 1. Principle of the triplexer structure.

Keywords

Triplex filter, multi-mode interference filter, directional coupler, WDM transceiver.

1. Introduction

During last twenty years photonics structures have played a key role in optical communication networks and optical sensor systems. Due to the rapid widespread of the optical communication equipment in the Fiber-to-the-Home (FTTH) networks a new planar photonics devices are strongly required [1-4]. Triplexing filter (triplexer) is generally used on the customer premise, which is capable to upload the data through 1310 nm channel, download internet data and voice data through the 1490 nm channel and to receive video signals through the 1550 nm channel, which are the wavelengths that are used according to the international TDM-PON ITU-T G.983 and G.984 standards. Principle of the triplexer structure is shown in Fig. 1.

Several papers dealing with optical triplexer fabricated by various design concept and different materials have appeared recently in the literature [5-10]. Reported devices were usually based on semiconductor or glass

For the thought purpose new polymers have lot of interesting properties such as temporal and temperature stability, high transparency from visible to infra-red wavelengths, well-controlled refractive indices, low optical losses, easy fabrication process etc. [11-14].

Planar optical wavelength selective systems with the triplex filter are intended to be used for WDM transceiver application in Passive Optical Network- Fiber to the x (PON-FTTx) topology [15]. Recent deployments of Fiber to the Home (FTTH) technology represent the fastest growing sector of the telecommunication industry. Fiber to the Home (FTTH) and Fiber to the Premise (FTTP) have growing opportunity for the world optical telecom market, bringing substantial gains in bandwidth directly to the end user.

In this paper we are going to describe already existing and new design solutions of the planar optical triplex filters for PON-FTTx application.

The triplex filter, which connects the direction coupler and arrayed waveguide grating (DC-AWG) [16], was made by deposition on Si/SiO₂. This material has very good wavelength selectivity and crosstalk, but it also suffers of higher insertion losses and lithographic difficulties requiring very accurate dimensions of coupling sections in AWG. Similar technological difficulties can be also found

in the case of a triplex filter with polarization insensitive two directional couplers (DC-DC), based on submicron silicon rib waveguides [17]. Total device length is about 400 μm , which is much shorter than already existing triplexers based on arrayed waveguide gratings (12 mm). Both triplex filters have dimensions of their channel optical waveguides below 1 μm , which come from high contrast index of refraction for used materials.

Planar triplex filters using thin-film filters (TFF) [15] are localized as optical taps filters along the optical planar waveguides in hybrid WDM transceiver. The hybrid design based on Si/SiO₂ means high demands on accuracy of technology and precision of construction.

Polymer optical cascade-step-size multimode interference filter (CSS-MMI filter) [18] is created by two-graded interference spaces on polymer 6701A and 5202A (from Rohm and Haas).

Comparison of insertion losses and crosstalk of the planar triplex filters together with the parameters of microoptical VHGT (Volume Holographic Grating Triplexer) element for optical bandwidth from 1310 nm to 1550 nm is given in Tab. 1. Obviously, VHGT has relatively low insertion losses associated with high diffraction efficiency and high diffraction angle, which imply short dimension of WDM transceiver, but the optical crosstalk is rather higher.

Triplex filter	DC-AWG	TFF	CSS-MMI	VHGT
Insertion loss (dB)	0.15 - 5	0.9	0.15-1.5	0.3 - 1.3
Crosstalk (dB)	35 - 45	18 - 22	15 -18.5	12.4 -18

Tab. 1. Insertion losses and crosstalk of different types of triplex filters.

In this paper we are going to report about a design of a novel planar polymer triplex filter consisting of a multimode interference (MMI) filter optically bound to a directional coupler (DC). For the construction of the optical MMI-DC triplex filter, we used planar optical integrated approach based on epoxy polymer NANOTM SU-8 2000 (SU8) supported by Micro Chem Corp. placed on the Si substrate with SiO₂ isolation layer and covered by Polymethylmetacrylate (PMMA). SU8 is epoxy-based photoresist designed for micromachining and other microelectronic and micro-optical applications, where a chemical and thermal stability is required. Film thickness from 0.5 μm to 200 μm can be achieved. The SU8 polymer has good optical and mechanical properties; the optical losses are less than 1 dB/cm for 1300/1550 nm wavelengths. The proposed triplex filter structure is schematically shown in Fig. 2.

The optical MMI-DC triplex filter was used for separation of downstream and upstream optical radiation in our designed planar hybrid integrated WDM transceiver (see later). The triplex filter separates two downstream optical signals with wavelengths $\lambda_1 = 1490$ nm and $\lambda_2 = 1550$ nm,

which propagate from PORT1 to PORT3 and PORT4, (see Fig. 2). Simultaneously the upstream optical signal $\lambda_3 = 1310$ nm is routed in the reverse direction from PORT2 to PORT1. Triplex filter was designed using Beam Propagation Method (BMP) by Beam PROPTM software from Rsoft Design Group Inc.

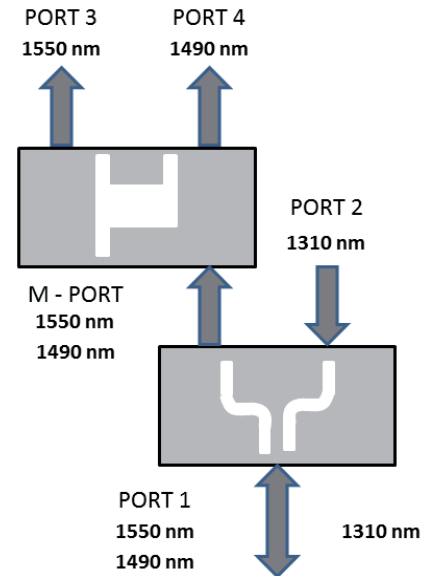


Fig. 2. The schematic configuration of designed MMI-DC triplex filter.

2. Theory

In this part of the paper we are going to derive formulas for estimation of interference length L_i and interference width W_i of MMI section. BMP program simulation procedure makes possible to optimize insertion losses and selectivity of the DC and MMI parts of MMI-DC triplex filter as well as a shape of the waveguides connection.

MMI device can be used as optical power splitter, power coupler or wavelength multiplexer. Actual operation of optical MMI devices is based on the self-imaging principle of the input optical field periodically recurring itself at beat lengths L_π in single or multiple images [19], [20].

Assuming two-dimensional representation in a lateral axis x , the condition of phase resonance can be described by the dispersion equation (1):

$$k_{xm}^2 + \beta_m^2 = k_0^2 n_{eff}^2 \quad (1)$$

where k_{xm} is the lateral wavenumber, β_m is the propagation constant, and n_{eff} is effective refractive index. Consequently, from (1) β_m is expressed as:

$$\beta_m = \sqrt{k_0^2 n_{eff}^2 - \left[\frac{(m+1)\pi}{W_e} \right]^2} \quad (2)$$

where the “effective” width W_e , takes into account the (polarization-dependent) lateral penetration depth of each

mode field, associated with the Goos-Hahnchen shifts at the ridge boundaries.

By using the binomial expression of (2) under condition (3), the propagation constant β_m can be deduced as approximation (4)

$$k_0^2 n_{eff}^2 \gg \left[\frac{(m+1)\pi}{W_e} \right]^2, \quad (3)$$

$$\beta_m \cong k_0 n_{eff} - \left[\frac{(m+1)^2 \pi \lambda_0}{4 n_{eff} W_e^2} \right]. \quad (4)$$

The length scale over which the multimode interference occurs is known as L_π , the beat length of the MMI region. By defining L_π as the beat length between the first two modes with phase difference π

$$L_\pi = \frac{\pi}{\beta_0 - \beta_1} \cong \frac{4 n_{eff} W_e^2}{3 \lambda_0}. \quad (5)$$

The propagation constants spacing can be written as

$$\beta_0 - \beta_m \cong \frac{m(m+2)\pi}{3L_\pi}. \quad (6)$$

The field profile at the distance L is therefore

$$\Psi(y, L) = \sum_{m=0}^{m-1} c_m \psi_m \exp \left[j \frac{m(m+2)^2 \pi}{3L_\pi} L \right]. \quad (7)$$

It can be seen from (7), that the original input can be completely reproduced (self-imaged), when the exponent term equals to one. This condition is satisfied with interference length L_I (8), where p is any integer parameter. When p is even, the image will be a direct one, when p is odd, the image will be mirrored.

$$L_I = p(3L_\pi). \quad (8)$$

Multiples (N-fold) images are then projected at length of

$$L_I = \frac{p}{N} (3L_\pi). \quad (9)$$

According to the above-mentioned MMI self-imaging theory, an input field in the MMI device can be reproduced along the MMI coupler at certain periodic intervals: $2p(kL_\pi)$ (bar state/direct image), and $(2p+1)(kL_\pi)$ (cross state/mirror image), respectively. In other words, because an MMI device can operate as a bar coupler for one wavelength and a cross coupler for the other wavelength, it can perform the signal separation between two wavelengths λ_1 and λ_2 . Therefore, the total length of the MMI device meets the following equation:

$$L_I = l(3L_{\pi, \lambda_1}) = q(3L_{\pi, \lambda_2}) \quad (10)$$

where l is even constant, q is odd constant and k is 3 for the general coupler and 1 for the restricted coupler.

Using the coefficients l and q it is possible to express reduction parameter k_{MMI} indicating the least common multiple, by which it is possible to multiply beat distances L_π so that the interference length is equal for both wavelengths (11).

$$k_{MMI} = \frac{9L_{\pi, \lambda_1} L_{\pi, \lambda_2}}{L_I} = \frac{3L_{\pi, \lambda_1}}{q} = \frac{3L_{\pi, \lambda_2}}{l}. \quad (11)$$

3. Design and Simulation Results

The insertion attenuations are specified by (12) and crosstalk attenuation by (13). The equations respect the signal propagation directions.

$$A_{1(\lambda_x)} = 10 \log \left(\frac{P_z}{P_y} \right), \quad (12)$$

$$A_{2(\lambda_x)} = 10 \log \left(\frac{P_z}{P_y} \right) \quad (13)$$

where $A_{1(\lambda_x)}$ in dB are insertion attenuations and $A_{2(\lambda_x)}$ in dB are crosstalk attenuations for wavelength λ_x , where $x = 1, 2, 3$ and $\lambda_1 = 1490$ nm, $\lambda_2 = 1550$ nm and $\lambda_3 = 1310$ nm. P_z is input optical power, where $z =$ PORT 1, PORT 2 or PORT M, P_y is output optical power, where $y =$ PORT 1, PORT M, PORT 3 or PORT 4 (see Fig. 1).

The design of DC coupler was made having in mind to minimize the crosstalk below 10 %. The calculations and simulations determined the parameters of DC coupler, which are listed in Tabs. 2 and 3. The calculations were done for refractive indices given in Tab. 4.

Insertion loss A_1	A_1	A_1	A_1
Output PORT	PORT 1	PORT M	PORT M
Input PORT	PORT 2	PORT 1	PORT 1
	(1310 nm)	(1490 nm)	(1550 nm)
DC coupler [dB]	0.36	0.43	0.32

Tab. 2. Insertion losses A_1 of the planar DC coupler for 1310 nm, 1490 nm and 1550 nm.

Crosstalk A_2	A_2	A_2
Output PORT	PORT 2	PORT 2
Input PORT	PORT 1	PORT 1
	(1490 nm)	(1550 nm)
DC coupler [dB]	14.5	11.35

Tab. 3. Crosstalk attenuation of the planar DC coupler for 1490 nm and 1550 nm to PORT 2.

Wavelength [nm]	Refraction indices		
	n_s [-]	n_f [-]	n_c [-]
1550	1.456	1.581	1.477
1490	1.456	1.581	1.477
1310	1.456	1.581	1.477

Tab. 4. Refraction indices for simulated polymer MMI-DC triplex filter, where n_s is refractive index of isolation layer, n_f is refractive index of waveguide layer, n_c is refractive index of cover layer.

Based on the results of the simulations the optimal offset value $L_o=6.5 \mu\text{m}$ to minimize crosstalk between PORT 2, PORT 3 and PORT 4 was set. Schematic view of DC (directional coupler) topology is shown in Fig. 3.

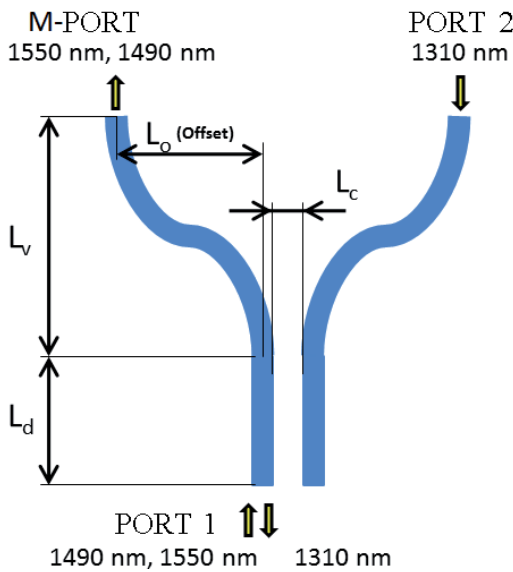


Fig. 3. Schematic view of DC (directional coupler), L_c is coupling gap, L_d is length of coupling, L_o is offset, L_v is separation distance, where PORT 1 is input for 1490 nm and 1550 nm and output for 1310 nm, PORT 2 is input for 1310 nm, and M-PORT is output for 1490 nm and 1550 nm.

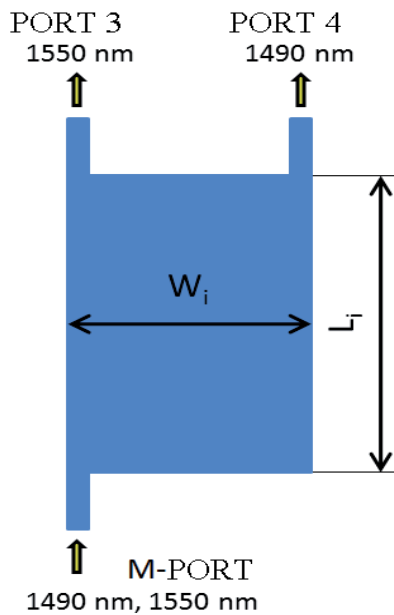


Fig. 4. Schematic view of MMI-interference filter, L_i is length of interference section, W_i is width of interference section, where M - PORT is input for 1490 nm and 1550 nm, PORT 3 is output for 1550 nm, PORT 4 is output for 1490 nm.

Design of the MMI filter was made again having in mind to minimize the crosstalk at least below 5 %. Schematic view of MMI filter topology is shown in Fig. 4. The calculations and simulations determined the parameters of the MMI filter. Design of the polymer wavelength splitter

1310 nm/1550 nm based on multimode interferences have been already presented in [21]. Parameters of the MMI filter are listed in Tabs. 5 and 6.

Insertion loss A_1	A_1	A_1
Output PORT	PORT 4	PORT 3
Input PORT	PORT M (1490 nm)	PORT M (1550 nm)
MMI filter [dB]	2.59	2.88

Tab. 5. Insertion losses of the planar MMI filter for 1490 nm and 1550 nm.

Crosstalk A_2	A_2	A_2
Output PORT	PORT 3	PORT 4
Input PORT	PORT M (1490nm)	PORT M (1550 nm)
MMI filter [dB]	14.81	16.3

Tab. 6. Crosstalk attenuation of the separated planar MMI filter for 1490 nm and 1550 nm.

The first step of the designing the thought direct coupler was using the parameters of the separated DC and MMI filter given in Tabs. 2, 3, 5 and 6 to approximate the idealized direct connection of both devices. The second step was minimizing of insertion losses and crosstalk by connecting of MMI and DC triplex filter and optimized the offset length L_c , which is half distance between MMI filter outputs for 1490 nm and 1550 nm and DC input for 1310 nm.

Schematic view of MMI-DC triplex filter topology is shown in Fig. 5.

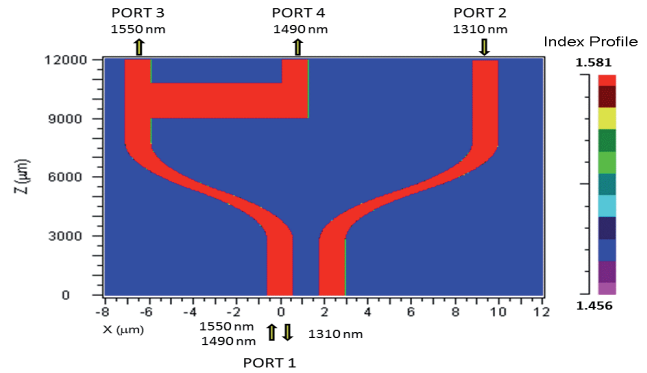


Fig. 5. Schematic view of MMI-DC triplex filter, where PORT 1 is input for 1490 nm and 1550 nm, and output for 1310 nm, PORT 2 is input for 1310 nm, PORT 3 is output for 1550 nm, PORT 4 is output for 1490 nm.

In the down stream the wavelengths 1490 nm and 1550 nm are routed from PORT 1 across DC and inter-connecting waveguide to PORT 4 and PORT 3 of MMI filter. In the reverse direction the wavelength 1310 nm is connected from PORT 2 of DC to PORT 1.

For the real structure of MMI-DC triplex filter we used the epoxy polymer SU8 optical ridge waveguides, which were deposited by spin coating method on Si/SiO₂ substrate. As a cover we used PMMA polymer (for the pertinent refraction indices see Tab. 4). High contrast of refraction indices implies low optical attenuation in a band

of optical waveguides. XY contour map cross-section profile of the polymer waveguide is shown in Fig. 6.

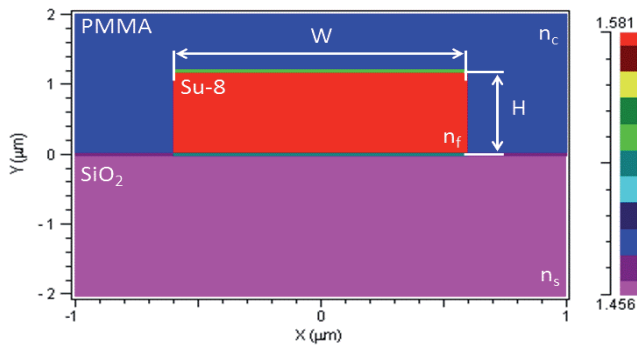


Fig. 6. XY contour map of the refractive index cross section for ridge optical polymer waveguides MMI-DC triplexer, where W is width and H is height of the waveguide core.

The optical radiation propagates along the planar polymer waveguide SU8 core layer with the refractive index $n_f = 1.581$. The substrate isolation layer of SiO₂ with $n_s = 1.456$ provides isolation of the core from Si substrate. The cover layer of PMMA with refractive index $n_c = 1.477$ prevents core layer and drop contrast of refraction indices (see Tab. 4).

The shape and dimensions of curve radius waveguides were set up to find optimal topology of MMI-DC triplex filter for 1310 nm, 1490 nm and 1550 nm. This way, optical insertion losses, crosstalk and spectrum selectivity were minimized by simulation in BMP software from RSoft. The 2D space distribution of the optical wave electrical field E_y for wavelength 1490 nm and monitor value E_y in the pathway is shown in Fig. 7. The left side shows the distribution of the electrical field in the XZ plane and the right side shows the relative amplitude of E_y for path way from PORT 1 to PORT 4. The insertion optical power transmission of MMI-DC triplex filter at 1490 nm corresponding to 52% was calculated.

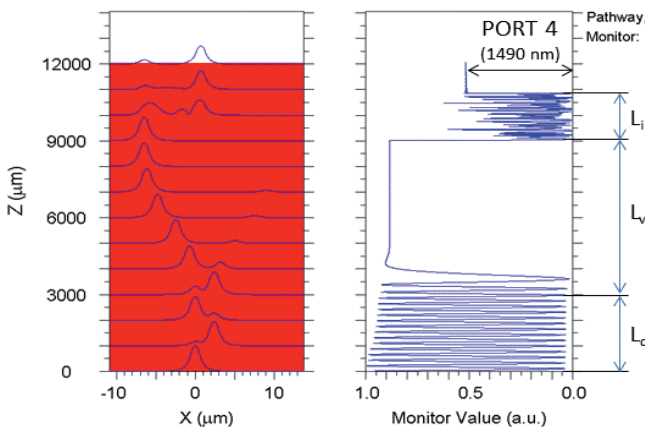


Fig. 7. 2D space distribution of the electrical field E_y for triplex filter in the plane XZ for 1490 nm (left side) and monitor value of E_y in the pathway from INPUT 1 to OUTPUT 4 (right side).

The 2D space distribution of the crosstalk electrical field E_y for wavelength 1550 nm in the path way from PORT 1 to PORT 4 is illustrated in Fig. 8. The crosstalk optical power transmission of MMI-DC triplex filter corresponding to 3 % was calculated.

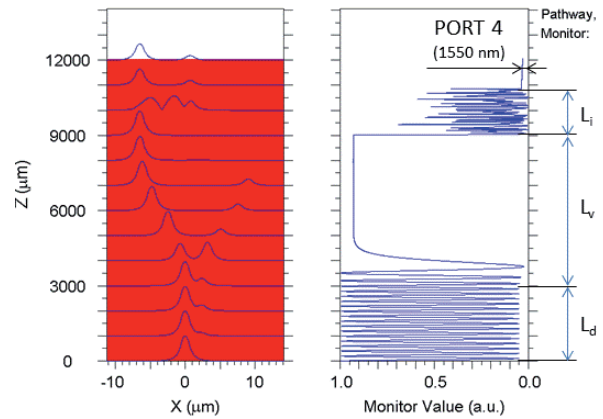


Fig. 8. 2D space distribution of the electrical field E_y for triplex filter in the plane XZ for 1550 nm (left side) and monitor value of E_y in the pathway from INPUT 1 to OUTPUT 4 (right side).

Spectral characteristics of MMI-DC triplex filter are given in Fig. 9 together with FWHM bandwidth of 15 nm for 1490 nm (Fig. 9a) and 16 nm for 1550 nm (Fig. 9b).

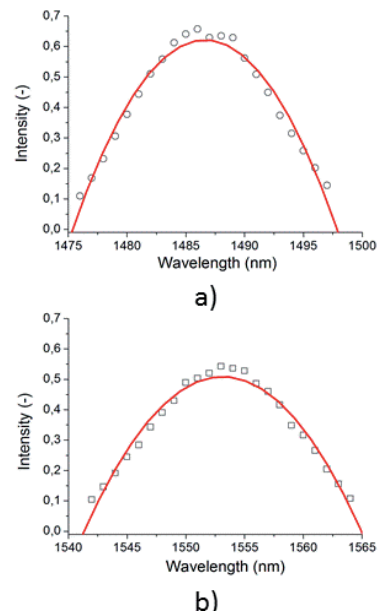


Fig. 9. Spectral characteristics of MMI-DC triplexer: a) PORT 1 to PORT 4 for 1490 nm, b) PORT 1 to PORT 3 for 1550 nm..

From optimized simulation we determined the optimal topology dimensions of MMI-DC triplexer (see Tab. 7) with assuming topological and optical field symmetry in the bilateral path way. The main parameters of direct connected and optimized MMI-DC triplex filter for wavelength 1310 nm, 1490 nm and 1550 nm are presented in Tabs. 8 - 10.

Topology constants	W	H	L_i	W_i
Devices dimensions [μm]	1.2	1.2	1833	8.4
Topology constants	L_d	L_v	L_c	L_o
Optimized triplex filter dimensions [μm]	2818	6200	1.2	6.5

Tab. 7. Optimized MMI-DC triplexer topological constants.

Insertion losses and crosstalk of the proposed MMI-DC triplex filter arises from optimization procedure of topological constants, where L_o and L_i had main influence. The optical power transmission of MMI-DC triplex filter were in the range between 0.48 and 0.68 after port number and the crosstalk power transmission got below value 0.07 for radiation at 1310 nm, 1490 nm and 1550 nm.

Insertion loss A_1 Output PORT Input PORT	PORT 1 PORT 2 (1310 nm)	PORT 4 PORT 1 (1490 nm)	PORT 3 PORT 1 (1550 nm)
Direct MMI-DC connection [dB]	0.36	3.02	3.2
Optim. triplexer connection [dB]	0.36	2.89	3.83

Tab. 8. The direct connected and optimized MMI - DC triplex filter insertion losses for 1310 nm, 1490 nm and 1550 nm.

The insertion losses parameters of the MMI-DC triplex filter are better for wavelength 1310 nm when comparing with the values at 1490 nm and 1550 nm. This is given by multimode function of MMI - DC elements, with serial connection, where optical power multipoint spreads in interference region.

Crosstalk A_2 Output PORT Input PORT	A_2 PORT 3 PORT 1 (1490 nm)	A_2 PORT 2 PORT 1 (1490 nm)	A_2 PORT 4 PORT 1 (1550 nm)	A_2 PORT 2 PORT 1 (1550 nm)
Direct MMI-DC connection [dB]	14.81	14.5	16.3	11.35
Optim. triplexer connection [dB]	15.19	17.8	14.29	11.79

Tab. 9. Direct connected and optimized MMI-DC triplex filter crosstalk attenuation for 1490 and 1550 nm.

Crosstalk A_2 Output PORT Input PORT	A_2 PORT 3 PORT 2 (1310 nm)	A_2 PORT 4 PORT 2 (1310 nm)
Optim. triplexer connection [dB]	36.4	36.4

Tab. 10. Optimized MMI-DC triplex filter crosstalk attenuation for 1310 nm.

The calculation of the least common multiple beat distances L_π and reduction parameter k_{MMI} from coefficients l and q , equation (11) are given in Tab. 11.

Symbol	L_1 [μm]	$3L_{\pi,1}$ [μm]	$3L_{\pi,2}$ [μm]	l	q	k_{MMI}
Values	1833.0	299.5	287.9	6.1	6.4	47.0

Tab. 11. Coefficients l , q and reduce coefficient k_{MMI} for mirror beat lengths L_π calculated for the MMI interference region.

The interference length of MMI-DC triplex filter with regard to minimization of insertion losses was optimized in

simulations, therefore the simulated interference length is smaller than the calculated one. The simulations revealed that the parameters l , q are not integers, and it is so due to the simplified conditions used in the derivation of the formula (5). The equation including the “effective” width W_e , which takes into account the (polarization-dependent) lateral penetration depth of each field mode associated with the Goos-Hahnchen, shifts at the ridge boundaries.

4. Application of MMI - DC Triplex Filter in Hybrid Integrated WDM Transceiver.

Our MMI-DC triplex filter is supposed to find its application in a planar hybrid integrated WDM transceiver shown in Fig. 10.

WDM transceiver consists of optical and optoelectronic part. The optical part is created by PLC (Planar Lightwave Circuit) of polymer MMI-DC triplex filter and SM fiber focus optics. For optical coupling of SM fiber to PLC it will be used optical taper element or optical grating coupler. As a polymer we choose the NANOTM SU8-2000 (SU8) polymer from Micro Chem Corp. for their good optical and mechanical properties as the polymer SU8 has optical attenuation less than 1 dB/cm for 1300 nm and 1550 nm.

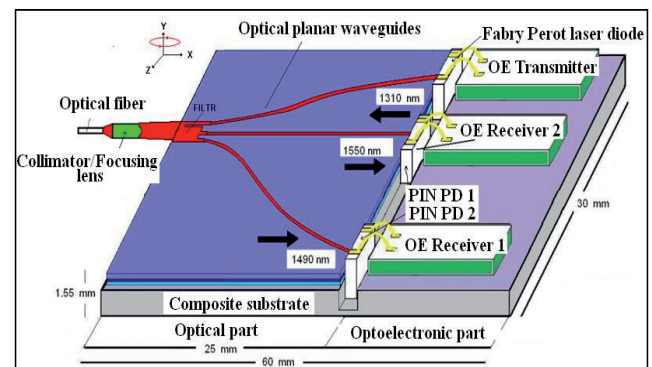


Fig. 10. Planar hybrid integrated WDM transceiver.

The optoelectronic part of WDM transceiver contains two OE receiver modules [22], with InGaAs PIN photodiodes (PD) and microwave amplifiers for down stream radiation 1490 nm and 1550 nm, optical bound at PORT 4 and PORT 3 of MMI filter. For upstream communication we used WDM transceiver OE transmitter module 1310 nm radiation, optical bounded from facet of Fabry-Perot InGaAsP laser diode (LD) to PORT 2 of MMI-DC triplex filter. OE transmitter has a microwave modulator and optical average power feed back control electronics of LD. The optoelectronic modules were made by thin layer hybrid integration technique. The optimum distance among optical waveguides facet on base polymer SU8 and SM optical fiber, PD or LD was specified by BMP program simulation.

5. Conclusion

To design a planar lightwave circuit MMI-DC triplex filter the polymer optical integrated technology was used. The dimensions of waveguides with inputs and outputs offset were set up to find optimal topology of MMI-DC triplex filter for 1310 nm, 1490 nm and 1550 nm. This way optical insertion losses, crosstalk and spectrum selectivity was minimized by simulation in BMP software from RSoft. The designed optimized insertion attenuation were $A_1=2.89$ dB and 3.83 dB for 1490 nm and 1550 nm. The insertion attenuation for 1310 nm was 0.36 dB and optical crosstalk was up to 11.8 dB. Spectral half-width characteristics of MMI-DC triplex filter were 15 nm for 1490 nm, 16 nm for 1550 nm and 2 nm for 1310 nm. By comparison of simulated parameters of separated MMI and DC elements, and farther optimization of the MMI-DC triplex filter, it is clear that by BMP package simulation parameters converged to the same dimensions and optical constants. The simulations of optical properties of MMI-DC triplex filters showed that MMI-DC triplex filter was sensitive in the order tenth of micrometers to the interference length L_i , width W_i and the coupling distance L_c of the DC element. These dimensions of MMI-DC triplex filter have to be set with micrometer accuracy. For implementation of our designed MMI-DC triplex filter with $1.2 \times 1.2 \mu\text{m}$ waveguides, the SU8 polymer technology with electron beam lithography was considered as the best approach. The proposed polymer MMI-DC triplex filter will be used in the designed optical part of planar hybrid WDM transceiver of PON optical networks.

Acknowledgements

This research has been supported by MPO-TIP grant FR-TI3/797 and the research program of the Czech Technical University in Prague, grant No. SGS13/080/OHK3/1T/13 and SGS11/156/OHK3/3T/13.

References

- [1] ZORTMAN, W. A., TROTTER, D. C., WATTS, M. R. Silicon photonics manufacturing. *Optics Express*, 2010, vol. 18, no. 23, p. 23598-23607.
- [2] JALALI, B., FATHPOUR, S. Silicon photonics. *Journal of Lightwave Technology*, 2006, vol. 24, no. 12, p. 4600-4615.
- [3] WONG, W. H., LIU, K. K., CHAN, K. S., PUN, E. Y. B. Polymer devices for photonics applications. *Journal of Crystal Growth*, 2006, vol. 288, no. 1, p. 100-104.
- [4] PRAJZLER, V., TŮMA, H., ŠPIRKOVÁ, J., JEŘÁBEK, V. Design and modeling of symmetric three branch polymer planar optical power dividers. *Radioengineering*, 2013, vol. 22, no. 1, p. 223-239.
- [5] BIDNYK, S., FENG, D., BALAKRISHNAN, A., PEARSON, M., GAO, M., LIANG, H., QIAN, W., KUNG, C. C., FONG, J., YIN, J., ASGHARI, M. SOI waveguide based planar reflective grating demultiplexer for FTTH. In *Proceedings of the Society of Photo-Optical Instrumentation Engineers (SPIE)*, 2007, p. 64770F-1 to 64770F-6.
- [6] LANG, T. T., HE, J. J., HE, S. L. Cross-order arrayed waveguide grating design for triplexers in fiber access networks. *IEEE Photonics Technology Letters*, 2006, vol. 18, no. 1-4, p. 232 - 234.
- [7] HUANG, W. P., LI, X., XU, Q., HONG, X., XU, C., LIANG, W. Optical transceivers for Fiber-to-the-Premises applications: System requirements and enabling technologies. *Journal of Lightwave Technology*, 2007, vol. 25, no. 1, p. 11-26.
- [8] SHI, Y. C., DAI, D. X., HE, S. L. Novel ultracompact triplexer based on photonic crystal waveguides. *IEEE Photonics Technology Letters*, 2006, vol. 18, p. 2293-2295.
- [9] SHI, Y. C., ANAND, S., HE, S. L. Design of a polarization insensitive triplexer using directional couplers based on submicron silicon rib waveguides. *Journal of Lightwave Technology*, 2009, vol. 27, no. 11, p. 1443-1447.
- [10] PRAJZLER, V., STRÍLEK, E., ŠPIRKOVÁ, J., JEŘÁBEK, V. Design of the novel wavelength triplexer using multiple polymer microring resonators. *Radioengineering*, 2012, vol. 21, no. 1, p. 258-263.
- [11] MA, H., JEN, A. K. Y., DALTON, L. R. Polymer based optical waveguides: Materials, processing and devices. *Advanced Materials*, 2002, vol. 14, no. 19, p. 1339-1365.
- [12] ELDADA, L. Optical communication components. *Review of Scientific Instruments*, 2004, vol. 75, no. 3, p. 575-593.
- [13] TUNG, K. K., WONG, W. H., PUN, E. Y. B. Polymeric optical waveguides using direct ultraviolet photolithography process. *Applied Physics A Materials Science & Processing*, 2005, vol. 80, p. 621-626.
- [14] PRAJZLER, V., KLAPUCH, J., LYUTAKOV, O., HÜTTEL, I., ŠPIRKOVÁ, J., NEKVINDOVÁ, P., JEŘÁBEK, V. Design, fabrication and properties of rib poly(methylmethacrylimide) optical waveguides. *Radioengineering*, 2011, vol. 20, no. 2, p. 479-485.
- [15] HAN, Y. T., PARK, Y. J., PARK, S. H., SHIN, J. U., LEE, C. W., KO, H., BAEK, Y., PARK, C. H., KWON, Y. K., HWANG, W. Y., OH, K. R., SUNG, H. Fabrication of a TFF-attached WDM-type triplex transceiver module using silica hybrid integration technology. *Journal of Lightwave Technology*, 2006, vol. 24, no. 12, p. 5031-5038.
- [16] AN, J. M., LI, J., LI, J. Y., WU, Y. D., HU, X. W. Novel triplexing-filter design using silica-based direction coupler and an arrayed waveguide grating. *Optical Engineering*, 2009, vol. 48, p. 014601-014601-4.
- [17] SHI, Y. C., ANAND, S., HE, S. L. Design of a polarization insensitive triplexer using directional couplers based on submicron silicon rib waveguides. *Journal of Lightwave Technology*, 2009, vol. 27, no. 11, p. 1443-1447.
- [18] FAN, S. H., GUIDOTTI, D., CHIEN, H. C., CHANG, G. K. A novel compact polymeric wavelength triplexer designed for 10 Gb/s TDM-PON based on cascade-step-size multimode interference. In *ECTC-Electronic Components and Technology Conference*, 2009, vol. 1-4, p. 220-223.
- [19] SOLDANO, L. B., PENNING, C. M. Optical multimode interference devices based on self-imaging: principles and applications. *Journal of Lightwave Technology*, 1995, vol. 13, no. 4, p. 615-627.
- [20] SAM, Y. L., WON, Y. H. A compact and low loss 1x2 wavelength mux/demux based on a multimode-interference coupler using quasi state. *Microwave and Optical Technology Letters*, 2004, vol. 41, no. 2, p. 86-88.

- [21] PRAJZLER, V., LYUTAKOV, O., HÜTTEL, I., ŠPIRKOVÁ, J., JEŘÁBEK, V. Design of polymer wavelength splitter 1310 nm / 1550 nm based on multimode interferences. *Radioengineering*, 2010, vol. 19, no. 4, p. 606-609.
- [22] JEŘÁBEK, V., ARMAS, J. A., PRAJZLER, V. Hybrid microoptical WDM receiver for PON communication. *Advances in Electrical and Electronic Engineering*, 2012, vol. 10, no. 2, p. 95-100.

About Authors ...

Vítězslav JEŘÁBEK was born in Prague in 1951. He received his PhD in Microelectronics from the Czech Technical University in Prague in 1987. From 2005 he is the head of optoelectronics group at the Department of Microelectronics, Czech Technical University in Prague. His research interests include planar hybrid integrated optics and optoelectronics devices.

Karel BUŠEK was born in Ceske Budejovice in 1976. In 2004 he graduated from the Faculty of Electrical Engi-

neering, Czech Technical University in Prague, Department of Microelectronics. His current research is focused on the design and investigation of properties of planar integrated optics.

Václav PRAJZLER was born in Prague, Czech Republic in 1976. In 2007 he obtained the PhD degree from the same university. His current research is focused on fabrication and investigation of properties of optical materials for photonics and integrated optics.

David MAREŠ was born in Melnik, Czech Republic in 1985. He received the M.Sc. degree from the Faculty of Electrical Engineering, Czech Technical University in Prague in 2012. His research interests include the design and investigation of properties of planar integrated polymeric nanostructures.

Rudolf SVOBODA was born in Pardubice in 1989. He obtained bachelor's degree at the Faculty of Electrical Engineering, CTU, Department of Microelectronics in 2011. His diploma thesis is focused on tunnel lighting.

RADIOENGINEERING REVIEWERS

December 2013, Volume 22, Number 4

- ABUELMA'ATTI, M. T., King Fahd University of Petroleum & Minerals, Saudi Arabia
- ARRIBAS, J., Centre Tecnològic de Telecomunicacions de Catalunya, Spain
- AYTEN, E. U., Yildiz Technical University, Turkey
- BARAN, O., Brno University of Technology, Czechia
- BARBOSA, G. M., Pontificia Universidade Católica do Rio de Janeiro, Brazil
- BECVAR, Z., Czech Technical University in Prague, Czechia
- BENETOS, E., City University London, UK
- BESTAK, R., Czech Technical University in Prague, Czechia
- BEZPALEC, P., Czech Technical University in Prague, Czechia
- BILIK, V., Slovak University of Technology, Bratislava, Slovakia
- BIOLEK, D., University of Defense, Brno, Czechia
- BLUMENSTEIN, J., Brno Univ. of Technology, Czechia
- BOLEČEK, L., Brno University of Technology, Czechia
- BRACHTENDORF, H.-G., University of Applied Science Upper Austria, Austria
- BRANČÍK, L., Brno Univ. of Technology, Czechia
- CAPEK, M., Czech Technical University in Prague, Czechia
- CATALDO, A., University of Salento, Italy
- CERNY, P., Czech Technical University in Prague, Czechia
- CHEN, H.-P., Ming Chi University of Technology, Taiwan
- CHENG, L., Trinity College, USA
- CIGANEK, J., Brno Univ. of Technology, Czechia
- COCHEROVA, E., Slovak University of Technology, Bratislava, Slovakia
- DIMITRIJEVIĆ, B., University of Niš, Serbia
- DOSTAL, T., Brno University of Technology, Czechia
- DROTAR, P., Brno University. of Technology, Czechia

- DŘÍNOVSKÝ, J., Brno University of Technology, Czechia
- EICHLER, J., Czech Technical University in Prague, Czechia
- FALCONE, F., Universidad Pública de Navarra, Spain
- FEDRA, Z., Brno Univ. of Technology, Czechia
- FISER, O., Academy of Sciences of the Czech Republic, Czechia
- GEIGER, B. C., Graz University of Technology, Austria
- GEORGIADIS, A., Centre Tecnologic de Telecomunicacions de Catalunya, Barcelona, Spain
- GLADIŠOVÁ, I., Technical University of Kosice, Slovakia
- GNING, A., University College London, UK
- GOKTEN, M., Türksat AS, Turkey
- GUTIÉRREZ, J., Universidad Politécnica de Madrid, Spain
- HAGARA, M., Slovak University of Technology, Bratislava, Slovakia
- HAJEK, K., University of Defense, Brno, Czechia
- HARTNAGEL, H. L., Technische Universität Darmstadt, Germany
- HAVLÍK, J., Czech Technical University in Prague, Czechia
- HAZDRA, P., Czech Technical University in Prague, Czechia
- HERENCŠAR, N., Brno University of Technology, Czechia
- HOFFMANN, K., Czech Technical University in Prague, Czechia
- HORSKY, P., ON Design Czech company, Czechia
- HORVATH, P., Budapest University of Technology and Economics, Hungary
- HOSSAIN, M. M., East West University, Bangladesh
- HUBÁLEK, J., Brno Univ. of Technology, Czechia
- HWANG, Y.-S., National Taipei University of Technology, Taiwan
- JAN, J., Brno University of Technology, Czechia
- JANOUŠEK, O., Brno Univ. of Technology, Czechia
- JELINEK, L., Czech Technical University in Prague, Czechia
- JENÍK, V., Czech Technical University in Prague, Czechia
- JERABEK, J., Brno Univ. of Technology, Czechia
- JIANG, T., Huazhong University of Science and Technology, China
- JUHÁR, J., Technical University of Kosice, Slovakia
- KABOUREK, V., Czech Technical University in Prague, Czechia
- KADLEC, P., Brno Univ. of Technology, Czechia
- KOLKA, Z., Brno Univ. of Technology, Czechia
- KOŘÍNEK, T., Czech Technical University in Prague, Czechia
- KOTON, J., Brno Univ. of Technology, Czechia
- KOUDELKA, V., Brno Univ. of Technology, Czechia
- KRACEK, J., Czech Technical University in Prague, Czechia
- KUBANEK, D., Brno Univ. of Technology, Czechia
- KUČERA, P., Pforzheim University, Germany
- KUMNGERN, M., King Mongkut's Institute of Technology Ladkrabang, Thailand
- KVATINSKY, S., Technion - Israel Institute of Technology, Israel
- LACIK, J., Brno Univ. of Technology, Czechia
- LAKKUNDI, V., Patavina Technologies, Italy
- LAMI, I., University of Buckingham, UK
- LEITGEB, E., Graz University of Technology, Austria
- LEVICKY, D., Technical University of Kosice, Slovakia
- LI, Y., Harbin Engineering University, China
- LOW, L., MIRA Ltd, UK
- LUKEŠ, Z., Brno Univ. of Technology, Czechia
- LUXEY, C., University of Nice-Sophia Antipolis, France
- MACHAJ, J., University of Zilina, Slovakia
- MARCHEVSKÝ, S., Technical University of Kosice, Slovakia
- MARTENS, R., University of Kiel, Germany
- MARTINEK, P., Czech Technical University in Prague, Czechia
- MASLENNIKOV, R., Lobachevski State University of Nizhny Novgorod, Russia
- MATSUNO, H., KDDI R&D Laboratories. Inc., Japan
- METIN, B., Bogazici University, Turkey
- MILOSEVIC, N., University of Niš, Serbia
- MEUNIER, J., University of Montreal, Canada
- MORÁVEK, O., Czech Technical University in Prague, Czechia
- MRÁZ, J., University of West Bohemia, Czechia
- MRKVICA, J., RETIA company, Czechia
- NIKOLIĆ, Z., University of Niš, Serbia
- NOUZA, J., Technical University of Liberec, Czechia

- OZEN, A., Nuh Naci Yazgan University, Turkey
- OZOGUZ, S., Istanbul Technical University, Turkey
- PANKRATZ, J. E., Silicon Laboratories, USA
- PETRZELA, J., Brno Univ. of Technology, Czechia
- PINCHAS, M., Ariel University Center of Samaria, Israel
- POLÁK, L., Brno Univ. of Technology, Czechia
- PRIBIL, J., Slovak Academy of Sciences, Slovakia
- PRIBILOVA, A., Slovak University of Technology, Bratislava, Slovakia
- PROMMEE, P., King Mongkut's Institute of Technology Ladkrabang, Thailand
- PROKES, A., Brno Univ. of Technology, Czechia
- PROKOPEC, J., Honeywell, Czechia
- PUSKELY, J., Brno Univ. of Technology, Czechia
- RADWAN, H., Cairo University, Egypt
- RAHIMIAN, A., University of Birmingham, UK
- RAMAHI, O., University of Waterloo, Canada
- ROBUSTILLO, P., Universidad Politécnica de Madrid, Spain
- ROVNAKOVA, J., Technical University of Kosice, Slovakia
- ROUABAH, K., University of Bordj Bou Arreridj, Algeria
- SCHIMMEL, J., Brno Univ. of Technology, Czechia
- SEBESTA, J., Brno Univ. of Technology, Czechia
- SEDIVY, P., RETIA company, Czechia
- SIAKAVARA, K., Aristotle Univ. of Thessaloniki, Greece
- SIGALOV, D., Technion - Israel Institute of Technology, Israel
- SIMEK, M., Brno Univ. of Technology, Czechia
- SIMSA, J., Academy of Sciences of the Czech Republic, Czechia
- SIPUS, Z., University of Zagreb, Croatia
- SIRIPRUCHYANUN, M., King Mongkut's University of Technology North Bangkok, Thailand
- SIZOV, V., University of Birmingham, UK
- SOTNER, R., Brno University of Technology, Czechia
- SPANEL, M., Brno Univ. of Technology, Czechia
- STELLA, M., University of Split, Croatia
- STORK, M., University of West Bohemia, Czechia
- SUN, X., Nanjing University of Information Science and Technology, China
- SYSEL, P., Brno Univ. of Technology, Czechia
- SZABÓ, Z., Czech Technical University in Prague, Czechia
- ŠEBESTA, V., Brno Univ. of Technology, Czechia
- ŠVANDA, M., Czech Technical University in Prague, Czechia
- TOMASIN, S., University of Padova, Italy
- TRALIC, D., University of Zagreb, Croatia
- ULOVEC, K., Czech Technical University in Prague, Czechia
- URBANEC, T., Brno Univ. of Technology, Czechia
- UŘIČÁŘ, T., Czech Technical University in Prague, Czechia
- VARGIC, R., Slovak University of Technology, Bratislava, Slovakia
- VENARD, O., ESIEE, Paris, France
- VERTAT, I., University of West Bohemia, Czechia
- VÍTEK, S., Czech Technical University in Prague, Czechia
- VLCEK, C., University of Defense, Brno, Czechia
- VODRAZKA, J., Czech Technical University in Prague, Czechia
- WIESER, V., University of Zilina, Slovakia
- WIKTOR, M., Medical University of Gdansk, Poland
- YANG, X.-S., University of Electronic Science and Technology of China, China
- YILMAZ, A. E., Ankara University, Turkey
- ZEKI, A., Girne American University, Turkey
- ZHANG, N., University of Florida and Maxlinear Inc., USA
- ZHAO, B., Tsinghua University, China
- ZHU, F., University of Kent, UK
- ZÁVODNÝ, V., Eldis Pardubice s.r.o., Czechia
- ZVANOVEC, S., Czech Technical University in Prague, Czechia